# PRNU-Based Image Alignment for Defective Pixel Detection

Christof Kauba, Andreas Uhl
Department of Computer Sciences, University of Salzburg, AUSTRIA
{ckauba,uhl}@cosy.sbg.ac.at

## Abstract

*Image alignment or registration is needed for many tasks. Conventional techniques are based on the image content. For forensic purposes where the characteristics of the image sensor itself are investigated, alignment has to be done based on the pixel grid the sensor used to capture the images. Biometric sensor analysis is one example for which this kind of alignment is needed. Our method utilises the photo response non uniformity (PRNU) fingerprint of the biometric sensor to align the images. At first the PRNU noise residual is extracted and enhanced. Then the shifts of the images are corrected by determining peaks in the normalised cross correlation results of the individual images. One possible use case where such aligned images are needed is the detection of sensor ageing related pixel defects in the scope of the biometric template ageing phenomenon but our approach can be useful for many other tasks in the field of biometric sensor analysis.*

## 1. Introduction

Image registration or alignment describes the process of transforming various images into a common coordinate system. Alignment of images is needed for many different purposes, not only in 2D but also in 3D. Examples are medical applications, biological imaging, computer vision and analysing satellite images. Alignment is necessary in order to be able to compare the data in different images. There is extensive literature [3, 13, 19] about different image registration techniques. Image registration algorithms can be classified into feature-based and intensity-based ones. They can be further classified into spatial domain and frequency domain methods. All of these methods have one thing in common: the alignment is somehow based on the image content. Image content in this case means the physical structures which are depicted in the images, e.g. a brain in medical images or objects in computer vision. Each image registration approach tries to extract features from the images, representing the image content and match the feature sets to find the correct correspondences between different images. The main purpose for doing image alignment or registration is analysis of the image data in form of the image content and thus all these methods are based on the image content to provide meaningful comparison results.

Image alignment, however, is needed in other application domains, e.g. in the context of biometrics if it comes to biometric sensor analysis, including analysis of the image sensor's characteristics with respect to different acquisition conditions, like stability, linearity of the output signal, etc. One specific application scenario is image sensor ageing investigation in the scope of the biometric template ageing phenomenon. This requires the detection and tracing of defective pixels inside the images. In a more general context image sensor analysis belongs to forensic image analysis which includes e.g. sensor identification/fingerprinting, forgery detection, tampering detection, device linking and image source identification [7]. In contrast to the conventional image registration techniques, in forensic image alignment the common coordinate system is the pixel grid originally used by the sensor at the time the image was acquired. The information at a certain pixel position inside the image has to originate from the same physical pixel on the image sensor grid in every image, which is totally different to aligning an image based on its content where the absolute pixel positions are not relevant. As we are working in the field of image sensor ageing in the context of biometric template ageing we needed a method to align images according to the physical pixel grid of the image sensor. After thorough literature research we were not able to find a suitable approach thus we decided to design our own one in order to do our image sensor ageing analysis.

Our image alignment approach is based on the photo-response non-uniformity (PRNU) which is an intrinsic property of each image sensor. Goljan and Fridrich proposed an approach for device identification from cropped and scaled pictures [8]. They use a brute force search to find the right scaling factor and the normalised cross correlation (NCC) to find the cropping parameters. We slightly modified their approach and use it for a different task, namely to do image alignment in the context of biometric sensor analysis. After extracting the noise residual from every image, the PRNU fingerprint of the image sensor is estimated. Based on this estimation all images are aligned according to one reference image. For alignment we use the NCC between the PRNU fingerprint of the sensor and the test image but in contrast to Goljan and Fridrich we use the maximum correlation value directly instead of the Peak to Correlation Energy (PCE) measure as it provided better results. PCE failed in correctly (pixel accurate) detecting the shifts.

The rest of this paper is organised as follows: Section 2 describes our PRNU based image alignment approach. Section 3 explains the performance evaluation using different biometric datasets. Section 4 provides an example use case - the detection of defective pixels in the images of the ND-Iris-Template-Aging-2008-2010 DB [1] which required image alignment in advance. Section 5 concludes this work.

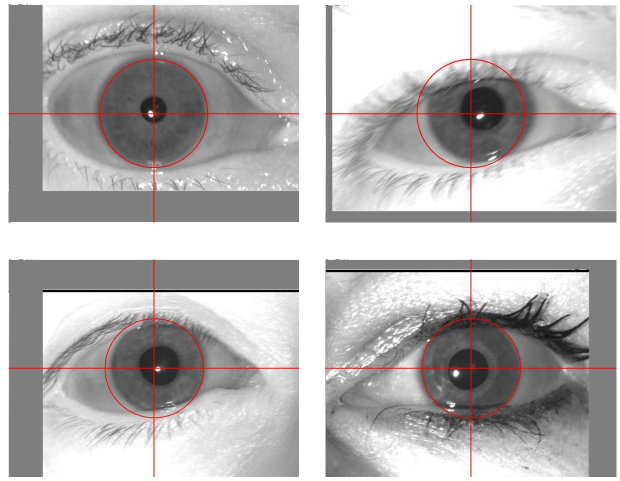

Figure 1. Iris image alignment based on the image content (iris centered)

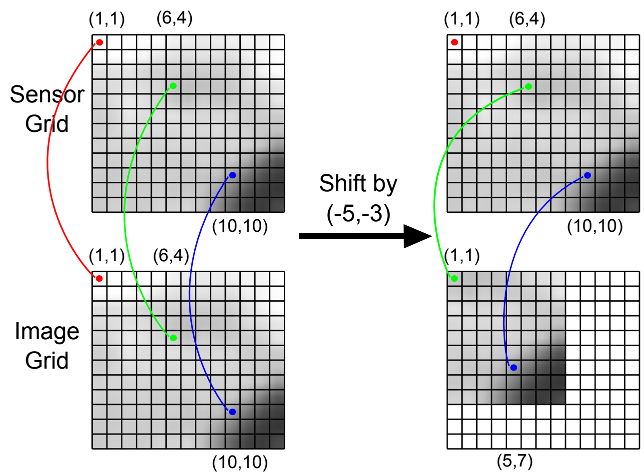


Figure 2. Shifted images with corresponding physical sensor grid pixel relations

## 2. PRNU Based Image Alignment

At first this section outlines the difference between conventional image alignment and the type of alignment needed in sensor forensics. Afterwards our image alignment approach based on the PRNU is explained. We follow the methodology of Goljan and Fridrich [8]. The extraction of the PRNU noise residuals, the PRNU enhancement and the estimation of the sensor's PRNU fingerprint are described. Then the estimation of the shifts using normalised cross correlation and the alignment of the images based on these estimations are explained.

### 2.1. Conventional Image Alignment

The main purpose of conventional image alignment or registration is aligning images based on the image content in order to be able to analyse data extracted from the image's content. An example are medical images which have to be aligned according to the body parts that are depicted in order to do measurements and comparisons. The alignment process tries to find some landmarks or feature points in both images and establish correspondences between these points. Based on these correspondences the parameters of a (affine) transformation are estimated and the images are aligned such that the body part of interest is located at the same pixel position in each of the images. Another example from iris recognition can be seen in Figure 1 where the images are aligned in a way that the centre of the iris is located approximately in the centre of the image (images fromND-Iris-Template-Aging-2008-2010 DB [1]).

### 2.2. Image Alignment for Biometric Sensor Analysis

Image alignment in sensor forensic context is different from conventional image alignment as it is not based on the image content but on the physical pixel grid of the image sensor itself. The aligned images have to be aligned such that a certain pixel in each image originates from the same pixel located at the physical sensor grid. Figure 2 shows an example. In an unshifted image, pixel $(1, 1)$ in the image corresponds to pixel $(1, 1)$ on the physical sensor grid. If the image is now shifted $5$ pixels to the left and $3$ pixels up, pixel $(1, 1)$ in the image corresponds to pixel $(6, 4)$ on the sensor grid. $(x, y)$ denotes the $x$- and $y$-position of the pixel, respectively.

Alignment of images based on the physical sensor grid cannot be done based on the image content as the content is not intrinsically related to the physical sensor grid. Suitable features that are inseparably linked to the physical pixel grid of the sensor and thus to the image sensor itself have to be used. The photo-response non-uniformity, also called PRNU is well known in the context of digital image forensics [7]. It represents a noise-like pattern which is an intrinsic property of all digital image sensors and results from slight variations in the sensitivity of individual pixels to photons of the incoming light due to im-

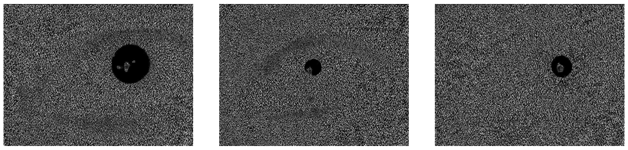

Figure 3. Example PRNU noise residuals

perfections in the manufacturing process. The PRNU is unique to each sensor, it is universal, i.e. every sensor has a PRNU, it is stable under a wide range of capturing conditions and it survives typical image processing operations (i.e. operations preserving the visual image quality) like lossy compression, filtering and white balance. Compression, scaling and low-pass filtering attenuate the PRNU but it does not completely disappear and can still be extracted. PRNU enhancement for these scenarios has been discussed thourougly in the PRNU-related forensic literature. The extraction of the PRNU is relatively easy using a denoising filter and a maximum likelihood approach if several images of the same sensor are available. PRNU based features can be utilised to do image alignment based on the physical pixel grid of the image sensor. Figure 3 shows some example PRNU noise residuals from two images taken by the same iris sensor (without shifts).

### 2.3. PRNU Extraction

The estimation of the PRNU fingerprint (where $W_I$ is the noise residual or PRNU fingerprint of a single image and $K$ is the PRNU fingerprint of the sensor) is done using the algorithm described by J. Fridrich [7]. The PRNU is basically noise which is introduced during the image acquisition process before the image is quantised or further processed. The following model describes the image sensor's output:

$$I = g^{\gamma} \cdot [(1+K)Y + \mathit{\Omega}]^{\gamma} + Q$$

where $I$ is the quantised sensor output signal, $Y$ is the incident light intensity, $g$ is the gain factor and $\gamma$ a correction factor, typically different for each colour channel. $K$ is a zero-mean noise-like signal representing the PRNU, $\mathit{\Omega}$ incorporates noise from other noise sources like dark current, shot noise and read-out noise and $Q$ is the combined distortion resulting from quantization and/or JPEG compression. $Y$ is the dominant term. By factoring out and keeping the first two parts of the Taylor series expansion we get:

$$I = (gY)^{\gamma} \cdot (1 + \gamma K + \gamma \mathit{\Omega}/Y) + Q = I^{(0)} + I^{(0)}K + \Theta$$

where we denote $I^{(0)} = (gY)^{\gamma}$ as the ideal sensor output if there is neither noise nor any imperfections. $I^{(0)}K$ is the PRNU term and $\Theta = \gamma I^{(0)}\mathit{\Omega}/Y + Q$ models the noise. The SNR of the signal of interest which is the PRNU term $I^{(0)}K$ and the image $I$ can be improved by suppressing the noiseless image $I^{(0)}$ through subtracting a denoised version of $I$, $\hat{I}^{(0)} = F(I)$ from both sides of the above equation using a suitable denoising filter:

$$W_I = I - F(I)$$

where $F$ is a denoising filter, filtering out the sensor pattern noise. $W_I$ is denoted as the noise residual of an image $I$. To extract the PRNU fingerprint, at first this noise residual is estimated. In this work we utilised the BM3D [5] denoising filter and the Wavelet-based denoising filter as described in Appendix A of [12] as they operate fast and produce good results in extracting the PRNU. Due to the nature of the PRNU it mostly covers the high frequency components of the image $I$. Thus it interferes with other high frequency components resulting from the image content itself, e.g. edges and fine structures. These lead to a less accurate estimation of the PRNU. J. Fridrich proposes to use images with a high luminance and smooth image content to calculate the PRNU in order to achieve a higher estimation accuracy. The accuracy also gets higher if not only one image is used to extract the PRNU but several images taken by the same sensor. The PRNU fingerprint $\hat{K}$ of a sensor can then be estimated using the maximum likelihood principle for images $I^i$ with $i = 1...N$:

$$\hat{K} = \frac{\sum_{i=1}^{N} W_I^i I^i}{\sum_{i=1}^{N} (I^i)^2}$$

Note that $\hat{K}$ contains all components that are systematically present in every images, i.e. artefacts introduced by JPEG compression, signal transfer and colour interpolation. While the PRNU is unique these artefacts may be shared among cameras of the same model. These artefacts are mainly periodic signals which can be suppressed as originally described by J. Fridrich [7]. In order to improve the results, the PRNU noise residual $\hat{K}$ is then normalised in respect to the L2-norm and a zero mean operation is applied. To suppress the periodic artifacts a Wiener filtering is performed in the Discrete Fourier Transform (DFT) domain. To further improve the results we apply a PRNU enhancement approach which aims at filtering out scene details using the following idea: Scene details contribute to the very strong signal components in the wavelet domain, so the stronger a signal component in the wavelet domain, the more it should be attenuated. The PRNU is transformed into the discrete wavelet transform (DWT) domain, where the enhancement function ELi, corresponding to the Model 3 proposed in [11] is applied to the coefficients. Afterwards the resulting coefficients are transformed back into the spatial domain by performing an inverse DWT (IDWT).

### 2.4. Image Alignment

As mentioned in the introduction the aim of our image alignment approach is not to align images according to the image content but according to the original pixel grid as captured by the sensor. This type of alignment can be used for forensic purposes, like biometric sensor analysis, in our presented example the detection of defective pixels caused by sensor ageing, which is explained in section 4. Let us assume that we have $N$ shifted images, all acquired using the same sensor. The images all have the same dimension, i.e. $w \times h$ pixels. The first step is the representation of each image $I$ by its PRNU fingerprint $W_I$. Therefore the PRNU noise residual is extracted using the approach described above. The next step is the estimation of the sensor's PRNU fingerprint $\hat{K}$. As the images are shifted by unknown shifts in $x$- and $y$-direction we cannot simply use all the images and calculate the maximum likelihood estimate. We have to find some images which are already aligned and use them as a starting point. This is done by calculating the normalised cross correlation (NCC) between the PRNU fingerprint of the $I$-th image $I_I$ and all other images $I_J$ for $J = 1...N$, $J \neq I$:

$$\rho_{[J,W_I]} = NCC(W_J, JW_I)$$

where $\rho$ is the correlation between the PRNU residual $W_J$ of image $J$ and the PRNU residual of the $I$-th image $W_I$ weighted by the image content of $J$ (optionally a window can be set, restricting the NCC calculation to a certain area of the PRNU in order to exclude the borders which improves the results in some cases). If $\rho$ is above a predefined threshold $\tau$ then the two images $I$ and $J$ are likely to be shifted equally. The maximum likelihood estimator for the sensor's PRNU fingerprint $\hat{K}$ is then calculated using all images where $\rho > \tau$:

$$\hat{K} = \frac{\sum_{i \in \{J | \rho_{[J,W_I]} > \tau\}}^{N} W_I^i I^i}{\sum_{i \in \{J | \rho_{[J,W_I]} > \tau\}}^{N} (I^i)^2}$$

If there are at least some hints about the shifts of the images available, the starting image $I$ should be an image with minimal shifts since in the next steps all images are aligned based on this image and the larger the shift differences are, the larger is the image area that is "lost" due to re-shifting the images. If no hints are available the first image is taken as reference image $I$ for simplicity. If there are no or only a small number of images $J$ for which the correlation value $\rho$ is above the threshold $\tau$, the next image $I = i + 1$ is taken as reference image and again the NCC scores are calculated (to find a suitable common basis).

After the estimation of $\hat{K}$, the normalised cross correlation (NCC) of all remaining images (not used during the estimation of $\hat{K}$) and the PRNU fingerprint $\hat{K}$ is calculated. The NCC calculates the correlation between the reference and the test image while the test image is circular shifted for all possible shifts in x- and y-direction. The NCC computes a matrix of correlation values $C_I$ for each image $I$

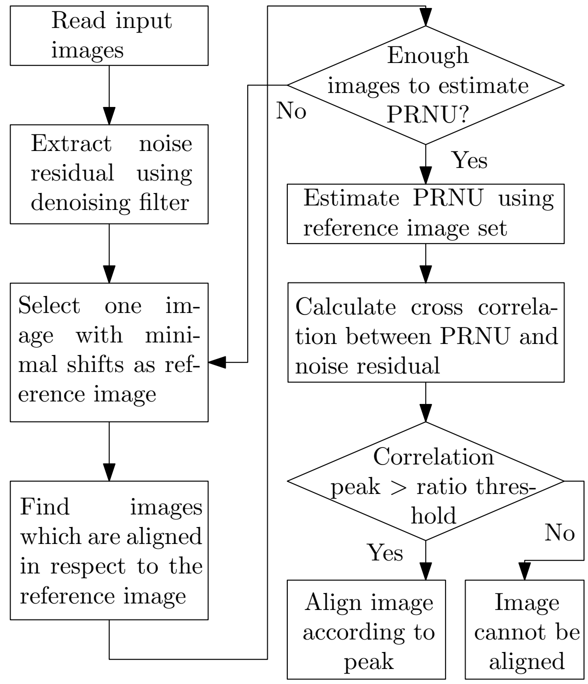


Figure 4. Flowchart of PRNU based image alignment

which has exactly the same size as the image, $w \times h$. The next step is to find the peak (maximum value) $\hat{c}_I$ in the matrix $C_I$. During our experiments it turned out that the maximum correlation value was more robust against outliers than the PCE (more images could be aligned correctly) and thus we decided to use the maximum correlation value instead of PCE. If the ratio $\frac{\hat{c}_I}{mean(c \in C_I)} > \gamma$ with the pre-defined threshold $\gamma$ holds, the correlation is distinguishable enough to be a valid peak. For images where this condition does not hold, the shifts cannot be reliably determined. For all other images the position $(x_{c_I}, y_{c_I})$ in the matrix $C_I$ where the peak $\hat{c}_I$ was found is used to re-shift the image:

$$I'(x, y) = I((x - x_{c_I}) mod(w), (y - y_{c_I}) mod(h))$$

where $I'$ is the aligned image (image which is shifted back to the sensor's original pixel grid), $x$ and $y$ are the horizontal and vertical pixel coordinates inside the image, respectively and $mod$ is the modulus operator. Depending on the further use of the images, they can either be circular shifted or the border can be filled up with black pixels.

Our approach is able to correct horizontal and vertical shifts present in the images. It can be extended to handle rotation and scaling in a similar way to the approach in [8]. Therefore the NCC calculation step has to be adopted to incorporate the calculation of the correlation values for rotated and scaled versions of the test image in addition to the shifted versions as NCC does. Of course this increases the computational demand depending on the granularity and the range of the rotations and scaling values.

## 3. Performance Analysis

To verify the accuracy of our proposed approach we did some simulations on various biometric datasets. The datasets and the simulation process are described below:

**UTFVP:** The University of Twente Vascular Pattern dataset [17] consists of 1440 near-infrared finger vein images. The images have a resolution of $672 \times 380$ pixels, captured with a custom build scanner.

**Vera PalmVein:** The Vera PalmVein dataset [16] consists of 1000 near-infrared palm vein images, having a resolution of $480 \times 640$ pixels, captured with a custom build scanner.

**Casia CrossSensor Iris:** We used a subset of the CASIA cross sensor iris database [18], consisting of 1500 images, having a resolution of $640 \times 480$ pixels. The subset contains only images captured with the Irisguard H100 IRT sensor as all images have to be from the same sensor.

**IITD:** The IIT Delhi iris dataset [9] consists of 1120 iris images, having a resolution of $320 \times 240$ pixels captured with a JIRIS, JPC1000, digital CMOS camera.

**FVC2002 DB1/DB2:** DB2 of the FVC2002 dataset [14] consists of 800 fingerprint images having a resolution of $296 \times 560$ pixels, captured with an optical fingerprint scanner (Biometrika FX2000). DB1 consists of 800 images, $388 \times 374$ pixels, captured with an optical fingerprint scanner (Identix TouchView II).

All images except the first one are shifted by random shifts in the range of $[-100, +100]$ pixel in horizontal and $[-60, +60]$ pixels in vertical direction for UTFVP, Vera Palmvein and Casia CrossSensor Iris (vice versa for portrait images) and $[-50 + 50]$ pixels in horizontal and $[-30, +30]$ pixels in vertical direction for IITD and FVC2002 DB2, respectively. Then our PRNU based image alignment approach is applied to the shifted images. The first image is selected as reference image during the alignment process. Afterwards the real shifts are compared with the determined ones. All simulations are run 10 times on each dataset and the results in the next section are the mean values of all runs. The following performance measures are calculated:

**Precision:** as for forensic purposes a pixel accurate alignment of the images is needed, this is the ratio of images which are aligned correctly ($\pm 0$ pixels) in x- and y-direction to all images in the dataset.

**Correlation:** Spearman correlation coefficient calculated between the actual and the determined shift values.

**MeanDeviation:** the mean of the Euclidian difference between the actual and the determined shifts.

Table 1 lists the results of our simulated image shift experiments. The results on the UTFVP, the Vera PalmVein and the FVC2002 DB2 dataset confirm that our approach is able to correctly detect the shifts and align all the images (except 1 for Vera Palm Vein). On the Casia CS iris it is still usable even if it fails to correctly align some of the images. For the IITD and the FVC2002 DB1 dataset our approach

| | Precision | Correlation | MeanDeviation | # failed |
|---|---|---|---|---|
| UTFVP | 1.0 | 1.0 | 0.0 | 0 |
| Vera PalmVein | 0.999 | 0.999 | 0.1068 | 0.9 |
| Casia CS Iris | 0.981 | 0.993 | 3.934 | 28.3 |
| IITD | 0.026 | 0.172 | 170.63 | 2181 |
| FVC2002 DB1 | 0.014 | 0.333 | 212.26 | 787.1 |
| FVC2002 DB2 | 1.0 | 1.0 | 0.0 | 0 |

Table 1. Performance evaluation results on the different datasets

completely fails. The main reason for this effect is assumed to be the size of the images. Both datasets have rather small images (less than $400 \times 400$ pixels). In combination with the high frequency image content (iris or fingerprint pattern, respectively) the extracted PRNU is not reliable enough.

The whole alignment process (i.e. reading the images, computing the PRNU, enhancing the PRNU, calculating the cross correlation and saving the aligned images) for the UTFVP images takes about $3390\,s$ with PRNU enhancement and and about $960\,s$ without it, respectively. For the smaller IITD images it takes $1650\,s$ w.E. and $423\,s$ without (assuming that all images except one need to be aligned).

## 4. Pixel Defect Detection

This section explains one of the possible applications for our PRNU based image registration approach. Image sensors develop defective pixels while they are in use. The most prominent defect types are hot and stuck pixels. These pixel defects are caused by damages in the silicon lattice due to the impact of cosmic ray radiation [15]. Pixel defects follow the once defective - always defective principle, i.e. once they appeared they do not heal and also their parameters do not change. Their locations follow a normal random distribution across the sensor area and inter-defect times follow an exponential distribution [10].

There are theoretical approaches to estimate the number of new defects a sensor will develop per year, i.e. the defect growth rate, like the empirical formula of Chapman et al. [4] but for more accurate estimates images captured by a sensor at different points in time with a time lapse of several years in between are needed. The first step is the detection of the defective pixels inside the images by statistical approaches, like the Bayesian approach by Dudas et al. [6] or the one by Bergmüller et al. [2]. After the defect locations and number of defects are known, the defect growth rate and the parameters of each single defect can be determined.

The most important requirement for the detection of the defective pixels is that a certain pixel position inside the image corresponds to the same physical position on the image sensor in every image. The statistical approaches to detect the defective pixels examine every image and estimate the probability, that a pixel at a certain position is defective depending on its characteristics compared to its neighbouring pixels. If the pixel is now shifted to a different position in every image, this probability is high for a single image but

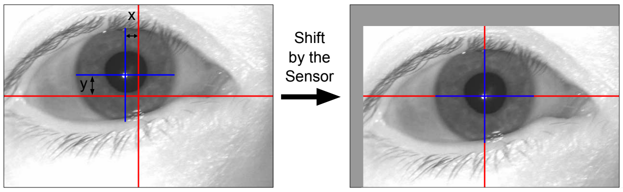


Figure 5. Image shifting introduced by the iris sensor

the overall probability across all images is low as the defective pixel at that position will most likely be a good one in the other images due to the shifts and thus not being recognised as defective one. Thus it is vital for an accurate and reliable detection of defective pixels that all the images are aligned pixel-wise according to the sensor' aoriginal pixel grid used during image capturing.

### 4.1. ND-Iris-Template-Aging-2008-2010

For our experiments regarding image sensor ageing effects in biometric recognition we evaluated the images of the ND-Iris-Template-Aging-2008-2010 database [1]. This database contains 3 sets of images, the first one captured in 2008, the second one in 2009 and the third one in 2010. Figure 1 shows some example images (the red lines and the circle have been added to indicate the centre of the image). One can clearly see the grey bars at the borders of the image. We found out that these are introduced by the iris sensor itself as it shifts the images (presumably to have the centre of the iris in the centre of the image), i.e. it takes the image, shifts it in a certain direction over the image borders and fills the now emerged missing pixels with grey bars. Figure 5 shows this process. At first we tested to re-shift the images by simply detecting the width of these bars and shift the image in the opposite direction to compensate the shifts. Afterwards we run the defect detection approach but the detection failed. Thus we assumed that shift compensation is not that easy and needs a more sophisticated approach.

Image alignment according to our proposed approach worked well for the 2008 and 2009 images but failed for some 2010 images. For these images there was no clear maximum correlation value and they were filtered out by the ratio threshold. We assume that in 2010, 2 sensors were used, the old one and an additional iris sensor. Some quick tests using one of the images where alignment failed as reference image and trying to align the other images based on this reference image worked for most of the images which previously could not been aligned. This is an indicator that indeed 2 sensors have been used in 2010. Figure 6 shows a schematic representation of the alignment procedure.

All images for which the alignment failed based on the 2008 reference image are not used to detect the defective pixels. After aligning the images, we were able to detect 12 hot pixels in the images of 2008, 13 in the images of 2009 and 13 in the 2010 images. 3 of the defects in 2008 were

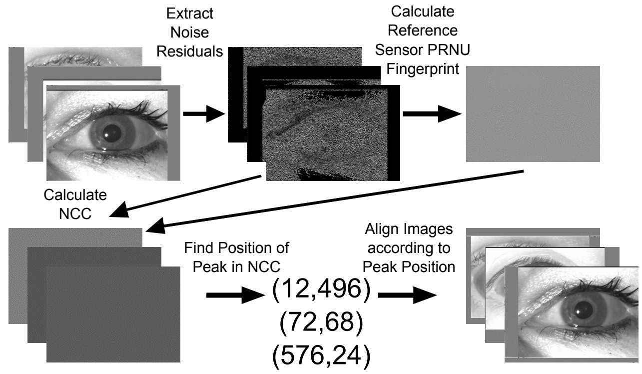


Figure 6. Image alignment procedure by the example of iris images

matching defects with 2009 and 2010 using the approach of Bergmüller et al. The approach proposed by Dudas et al. did not find any hot or stuck pixel defects. We masked out the inner area (where the iris texture is located) to get more accurate results. Figure 7 shows the detected defects inside the iris images for 2008, 2009 and 2010 as red pixels (only a part of the whole image for better visualisation, thus not showing all defective pixels). This yields a hot pixel defect growth rate of ($MP$ denotes Megapixels):

$$\lambda = 0.66725 \;\; defects/MP/year$$

which is in accordance to other results reported in the literature [2, 4, 10]. We used this estimated defect rate as a basis to analyse the impact of image sensor ageing related pixel defects on the performance of iris recognition systems following the approach of Bergmüller et al. by using a sensor ageing simulation algorithm.

## 5. Conclusion

We propose a new image alignment approach for biometric sensor analysis which aligns the images according to the physical pixel grid of the sensor. In contrast to the existing image registration methods, our approach is based on the PRNU fingerprint of the image sensor. At first the noise residual of every image is extracted. Then the PRNU fingerprint is estimated based on the noise residuals from images which are either not misaligned or misaligned in the same way. Afterwards all other images are aligned based on the PRNU fingerprint of the reference image(s). This approach is suitable for forensic image analysis, especially for biometric sensor analysis whenever the exact pixel positions inside the images have to match. We showed the good performance of our approach utilising artifically shifted images for 5 biometric datasets. As long as the images are of sufficient size the alignment works well. We also showed the effectiveness of our approach at the detection of defective pixels caused by image sensor ageing in the scope of biometric template ageing. Our approach needs at least $2-5$

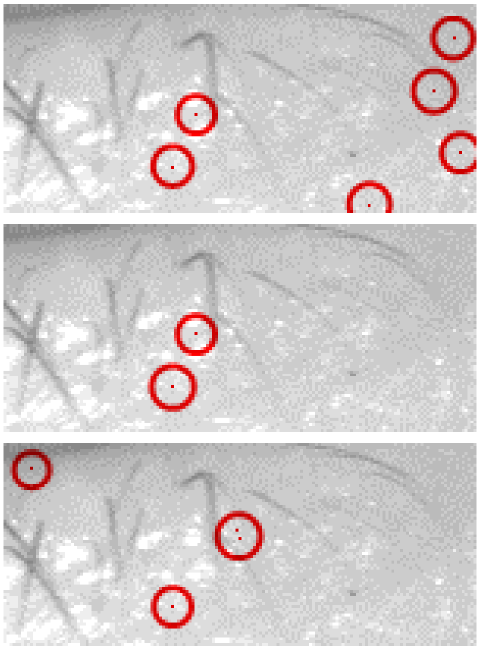

Figure 7. Detected hot pixel defects (from top to bottom: 2008, 2009 and 2010)

images for a reliable estimate of the sensor's PRNU fingerprint and thus to be able to correctly align the images. But for a reliable detection of defective pixels at least 50 images are needed to get meaningful results. We were able to align the images of the ND-Iris-Template-Aging database which were originally shifted by the iris sensor. This enabled us to detect the defective pixels in order to calculate the defect growth rate. This is only one of the possible applications in the area of biometric sensor analysis for which our approach has proven useful. As suggested it can be extended to handle rotation and scale variations in the images too.

## Acknowledgements

This work has been partially supported by the Austrian Science Fund FWF, project P26630. We thank Xufeng Lin who supported us in the discussion of the PRNU related parts during his STSM in the scope of COST Action IC1106.

## References

[1] S. E. Baker, K. W. Bowyer, and P. J. Flynn. Empirical evidence for correct iris match score degradation with increased time-lapse between gallery and probe matches. In *Proceedings of the Third International Conference on Advances in Biometrics*, ICB '09, pages 1170–1179, Berlin, Heidelberg, 2009. Springer-Verlag.

[2] T. Bergmüller, L. Debiasi, Z. Sun, and A. Uhl. Impact of sensor ageing on iris recognition. In *Proceedings of the IAPR/IEEE International Joint Conference on Biometrics (IJCB'14)*, 2014.

[3] L. G. Brown. A survey of image registration techniques. *ACM computing surveys (CSUR)*, 24(4):325–376, 1992.

[4] G. H. Chapman, R. Thomas, Z. Koren, and I. Koren. Empirical formula for rates of hot pixel defects based on pixel size, sensor area, and iso. In *IS&T/SPIE Electronic Imaging*, pages 1–12. International Society for Optics and Photonics, 2013.

[5] K. Dabov, A. Foi, V. Katkovnik, and K. Egiazarian. Image denoising with block-matching and 3d filtering. In *Electronic Imaging 2006*, pages 606414–606414. International Society for Optics and Photonics, 2006.

[6] J. Dudas, L. M. Wu, C. Jung, G. H. Chapman, Z. Koren, and I. Koren. Identification of in-field defect development in digital image sensors. In *Electronic Imaging 2007*, pages 1–12. International Society for Optics and Photonics, 2007.

[7] J. Fridrich. Digital image forensics. *Signal Processing Magazine, IEEE*, 26(2):26–37, 2009.

[8] M. Goljan and J. Fridrich. Camera identification from cropped and scaled images. In *Proc. SPIE, Electronic Imaging, Forensics, Security, Steganography, and Watermarking of Multimedia Contents X*, pages 1–13, 2015.

[9] A. Kumar and A. Passi. Comparison and combination of iris matchers for reliable personal authentication. *Pattern recognition*, 43(3):1016–1026, 2010.

[10] J. Leung, G. H. Chapman, Z. Koren, and I. Koren. Statistical identification and analysis of defect development in digital imagers. In *IS&T/SPIE Electronic Imaging*, pages 1–12. International Society for Optics and Photonics, 2009.

[11] C.-T. Li. Source camera identification using enhanced sensor pattern noise. *IEEE Transactions on Information Forensics and Security*, 5(2):280–287, 2010.

[12] J. Lukas, J. J. Fridrich, and M. Goljan. Digital camera identification from sensor pattern noise. *IEEE Transactions on Information Forensics and Security*, 1(2):205–214, 2006.

[13] J. A. Maintz and M. A. Viergever. A survey of medical image registration. *Medical image analysis*, 2(1):1–36, 1998.

[14] D. Maio, D. Maltoni, R. Cappelli, J. L. Wayman, and A. K. Jain. Fvc2002: Second fingerprint verification competition. In *Pattern recognition, 2002. Proceedings. 16th international conference on*, volume 3, pages 811–814. IEEE, 2002.

[15] A. J. Theuwissen. Influence of terrestrial cosmic rays on the reliability of ccd image sensors-part 1: Experiments at room temperature. *Electron Devices, IEEE Transactions on*, 54(12):3260–3266, 2007.

[16] P. Tome and S. Marcel. On the vulnerability of palm vein recognition to spoofing attacks. In *The 8th IAPR International Conference on Biometrics (ICB)*, May 2015.

[17] B. Ton and R. Veldhuis. A high quality finger vascular pattern dataset collected using a custom designed capturing device. In *International Conference on Biometrics, ICB 2013*. IEEE, 2013.

[18] L. Xiao, Z. Sun, R. He, and T. Tan. Coupled feature selection for cross-sensor iris recognition. In *Biometrics: Theory, Applications and Systems (BTAS), 2013 IEEE Sixth International Conference on*, pages 1–6. IEEE, 2013.

[19] B. Zitova and J. Flusser. Image registration methods: a survey. *Image and vision computing*, 21(11):977–1000, 2003.